Direct Calculation of Electron Transfer Parameters through Constrained Density Functional Theory

Qin Wu* and Troy Van Voorhis

Department of Chemistry, Massachusetts Institute of Technology, Cambridge, Massachusetts 02139

Received: March 24, 2006; In Final Form: June 6, 2006

It is shown that constrained density functional theory (DFT) can be used to access diabatic potential energy surfaces in the Marcus theory of electron transfer, thus providing a means to directly calculate the driving force and the inner-sphere reorganization energy. We present in this report an analytic expression for the forces in constrained DFT and their implementation in geometry optimization, a prerequisite for the calculation of electron transfer parameters. The method is then applied to study the symmetric mixed-valence complex tetrathiafulvalene−diquinone radical anion, which is observed experimentally to be a Robin−Day class II compound but found by DFT to be in class III. Constrained DFT avoids this pitfall of over-delocalization and provides a way to find the charge-localized structure. In another application, driving forces and inner-sphere reorganization energies are calculated for the charge recombination (CR) reactions in formanilide−anthraquinone (FA-AQ) and ferrocene−formanilide−anthraquinone (Fc-FA-AQ). While the two compounds have similar reorganization energies, the driving force in FA-AQ is 1 eV larger than in Fc-FA-AQ, in agreement with experimental observations and supporting the experimental conclusion that the anomalously long-lived FA−AQ charge-separated state arises because the electron transfer is in the Marcus inverted region.

1. Introduction

Electron transfer (ET) is a fundamental chemical reaction that impacts a variety of chemical systems, from biology to electronic devices. Energy transfer processes in photosynthesis and several other biological reactions go through electron transfer,[1] while ET in chemical reactions can also couple with proton transfer.[2,3] Meanwhile, heterogeneous ET reactions play a key role in dye-sensitized solar cells,[4] and modern research in molecular electronics mostly amounts to control of ET in various units.[5] These applications have generated a vast literature that testifies to the importance of ET. (See, for example, the five-volume series edited by Balzani[6] and numerous review articles.[7−11])

The temperature-dependent kinetics of electron transfer is characterized in classical Marcus theory[7,8,12−14] with two important parameters: the driving force and the reorganization energy. Two parabolas along a reaction coordinate can be used to represent the free energy curves of reactant and product states, as shown in Figure 1, and these two surfaces are defined by two parameters: the driving force is $-\Delta G°$, and λ is the reorganization energy. Anharmonic effects are also studied by a number of authors[15,16] but are not addressed in this work. In the diabatic representation, the two curves cross, and the crossing point (q_c) is the transition state. With the assumption that both parabolas have the same curvature, the activation energy, $\Delta G^{\ddagger}$, is given by

$$\Delta G^{\ddagger} = \frac{(\lambda + \Delta G°)^2}{4\lambda} \tag{1}$$

which then can be used in the Arrhenius relationship for the rate constant

$$k_{ET} = A \exp(-\Delta G^{\ddagger}/k_B T) \tag{2}$$

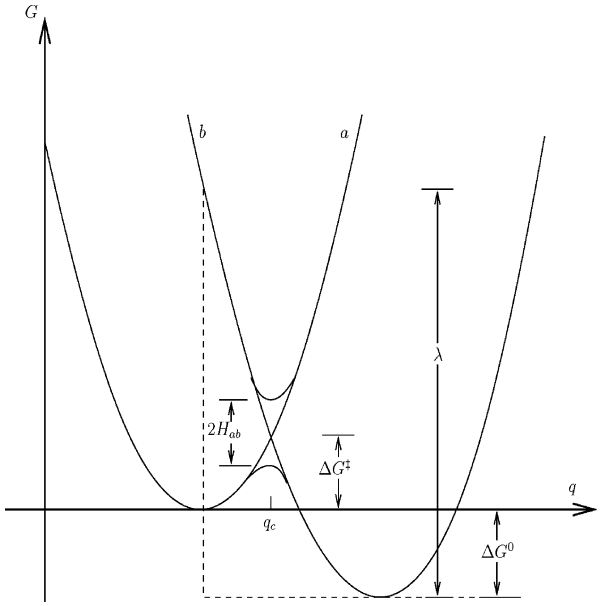

Figure 1. Potential energy curves of an electron transfer reaction. q represents the reaction coordinate.

where k_B is the Boltzmann constant. Note that eq 2 is essentially classical, and the temperature dependence of eq 2 breaks down when quantum effects are important.[17] In the adiabatic representation, the two curves avoid crossing, forming an upper and a lower curve with the energy gap at q_c being twice the electronic coupling constant H_{ab}. Figure 1 shows the potential energy curves in the limit of small H_{ab}, i.e., nonadiabatic transition, where the adiabatic curves differ from diabatic ones only in the region very near q_c. Most long-range ET studies are in this limit.

Ab initio quantum chemistry methods are now often used to calculate the ET parameters. Though free energies should be

10.1021/jp061848y CCC: $33.50
Published on Web 07/06/2006

used in real systems, in ab initio calculations entropy changes are often neglected, and instead, the potential energy is used. When the structures of the reactant and the product are exactly known, $\Delta G°$ is straightforwardly calculated as the difference of their equilibrium energies. Calculation of λ is more difficult, however, because it involves nonequilibrium energies. As seen in Figure 1, the reorganization energy is the energy decrease when the product state is relaxed from the reactant's equilibrium structure to its own equilibrium structure. λ is usually decomposed into an inner-sphere (λ_i) part and an outer-sphere (λ_o) part.[14] λ_i results from the structural changes of the reacting molecules, while λ_o is due to the solvent relaxation. For a gas-phase reaction, λ_i will be the only reorganization energy. But for reactions in solution or in a complicated biological environment, λ_o becomes dominant. Ab initio calculations are usually used to determine the inner-sphere reorganization energy. The most commonly used method is Nelsen's four-point method.[18] It treats the reorganization of the electron donor and acceptor separately. While this is an accurate approximation for intermolecular ET where the changes in the donor have nearly no effect on the acceptor and vice versa, it becomes less appropriate when the donor and the acceptor are connected and interact with each other.[19,20] It is possible to add a correction to the four-point method[21] to account for the donor−acceptor interaction, but a direct method that does not separate the donor and acceptor is much more desirable. Because of the large number of degrees of freedom involved in the outer-sphere reorganization, λ_o can often be simulated classically. One approach is to treat the solvent as a continuous dielectric medium characterized by a dielectric constant, with the reacting molecules sitting inside a vacuum cavity in the continuum.[22,23] Methods to calculate λ_o range from the simple formula of Marcus[7,12] to more sophisticated nonequilibrium models.[24,25] Further complication comes when the solvent plays a role more than electrostatically, such as forming hydrogen bonds with solute, for which solvent molecules have to be considered explicitly.[26] In this work, we will focus on the calculation of λ_i, leaving the outer-sphere component of the reorganization for future work.

The reason that it is difficult for ab initio methods to directly calculate λ_i is because it is not a ground-state property. In the adiabatic representation, as is usually produced by ab initio methods, the lower potential energy curve is of the ground state, while the upper one is of an excited state. To calculate λ_i, one needs the energy of the product state at the reactant state's equilibrium structure, which is the energy of a charge transfer (CT) excited state. Excited-state energies are generally much harder to compute accurately than the ground-state energy. Time-dependent density functional theory (TDDFT) methods are very promising,[27−29] giving good excited-state energies for relatively large systems (e.g., up to 100 atoms). However, the energy of long-range CT states given by TDDFT is largely underestimated,[30−34] which limits the usefulness of TDDFT in ET reactions.

Unlike the adiabatic states, diabatic states do not diagonalize the electronic Hamiltonian, and they are not readily available from ab initio calculations. There are two general ways to construct diabatic states (or quasidiabatic states, since strictly diabatic states generally do not exist[35−37]). One is to minimize the nuclear derivative coupling term,[38−40] which requires prior knowledge of nonadiabatic couplings. The other is to define diabatic states as those that have a similar electronic configuration at all nuclear coordinates. The latter is especially relevant in ET reactions where reactant and product states have different charge localizations. For instance, in a charge separation process, an electron transfers from the donor (D) to the acceptor (A); hence, DA is one of the diabatic states and D^+A^- is the other. For electron (hole) shifting, D^-A (D^+A) and DA^- (DA^+) then form the two diabatic states. There are a variety of approaches[41−48] to constructing diabatic states from an electronic structure technique, mostly from results of multiconfiguration ab initio calculations. In the diabatic representation, the reactant and product states can be treated on an equal footing. Here, we propose the use of constrained DFT as an alternative means of accessing diabatic states in ET reactions.

To obtain an ET diabatic state, one wants to explicitly constrain the electron density to the corresponding configuration (e.g., D^+A^- or DA) and carry out all calculations under the constraint. This constraint can be enforced by applying an appropriate extra external potential in the system,[49] where the key is to find out the correct constraining potential that gives the desired state.[50,51] Recently, we have implemented this constrained optimization[52,53] within Kohn−Sham DFT and successfully applied the method to long-range charge-separated states. We will present in this report how forces in constrained DFT can be calculated analytically, which leads to efficient geometry optimization of *diabatic* states from an essentially ground-state formalism. Having the equilibrium structures of both reactant and product states, one can then directly calculate the driving force and the inner-sphere reorganization energy.

In the rest of this report, we first briefly review the constrained DFT method, followed by a description of how analytic forces are calculated. We test the method first in the intervalence transfer of tetrathiafulvalene−diquinone radical anion, a symmetric mixed-valence compound that is treated poorly by unconstrained DFT. Then, the method is applied to calculations of the driving force and inner-sphere reorganization energies for formanilide−anthraquinone and ferrocene−formanilide−anthraquinone, where an unusual long-lived charge-separated state is observed in the former and is attributed to the inverted region of Marcus theory. In both cases, our constrained calculations support the experimental observations, while traditional DFT methods fail.

2. Method

2.1. Constrained DFT. The constrained DFT method was first proposed by Dederich et al.[49] It is based on the density functional theory of Hohenberg, Kohn, and Sham,[54,55] which says that the ground-state energy is given by the minimum of the following functional

$$E[\rho] = 2\sum_i^{N/2}\left\langle \phi_i \middle| -\frac{1}{2}\nabla^2 \middle| \phi_i \right\rangle + \int \mathrm{d}\mathbf{r}\, v_n(\mathbf{r})\rho(\mathbf{r}) + J[\rho] + E_{xc}[\rho] \quad (3)$$

where J is the classical Coulomb energy, E_{xc} is the exchange-correlation energy, and v_n is the external potential. N is the total number of electrons, and $\rho(\mathbf{r})$ is the electron density, $\rho(\mathbf{r}) = 2\sum_i^{N/2}|\phi_i(\mathbf{r})|^2$, with ϕ_i being the lowest-energy orbitals of a reference noninteracting system. For completeness, we briefly review the important formulas for computing energies in constrained DFT. For simplicity, we present here the formalism for closed-shell systems with a spin-restricted treatment. Our earlier work has general formulas for unrestricted cases.[52]

If a constraint on the electron density, e.g.,

$$\int w_c(\mathbf{r})\rho(\mathbf{r})\,\mathrm{d}\mathbf{r} = N_c \quad (4)$$

is applied, a constraining potential, V_c, can be introduced as

the Langrange multiplier so that minimizing the energy of the system subject to the constraint (eq 4) is equivalent to finding the stationary point of

$$W[\rho, V_c] = E[\rho] = V_c(\int w_c(\mathbf{r})\rho(\mathbf{r})\,d\mathbf{r} - N_c) \quad (5)$$

with respect to ρ and V_c. The stationary condition for V_c is just the constraint of eq 4, while the stationary conditions for orbitals are

$$\left[-\frac{1}{2}\nabla^2 + v_n(\mathbf{r}) + \int \frac{\rho(\mathbf{r}')}{|\mathbf{r}-\mathbf{r}'|}\,d\mathbf{r}' + v_{xc}(\mathbf{r}) + V_c w_c(\mathbf{r})\right]\phi_i = \epsilon_i\phi_i \quad (6)$$

which are the standard KS equations with an additional constraining potential, $V_c w_c(\mathbf{r})$, in the effective Hamiltonian. Early applications lacked a way to solve V_c and ϕ simultaneously, but we have recently developed a direct method to solve for V_c and ϕ in one self-consistent-field (SCF) calculation.[52]

For charge transfer, it is most convenient to constrain the charge difference between the donor and the acceptor; that is, $N_c = (N_D - N_A)/2$, where N_D and N_A are the net charges on D and A.[52,53] This can be done by defining the weight function in eq 4 to be positive on the donor and negative on the acceptor, which effectively constrains both the donor and the acceptor. As in implementations of most quantum chemistry codes, a set of atom-centered basis functions is used to expand ϕ_i, $\phi_i(\mathbf{r}) = \sum_\mu c_{\mu i}\chi_\mu(\mathbf{r})$, and energy is then in terms of the density matrix $\mathbf{P}$. We also build a weight matrix $\mathbf{w}_c$ in our calculations so that eq 5 is rewritten as

$$W[\mathbf{P}] = E[\mathbf{P}] + V_c(\mathrm{Tr}\{\mathbf{P}\mathbf{w}_c\} - N_c) \quad (7)$$

where Tr stands for the matrix trace. Among different schemes to define the weight matrix, we found that the Löwdin population often gives satisfactory results for long-range charge transfer states.[53] Elements of the Löwdin weight matrix are given by

$$w^L_{c\lambda\nu} + \sum_{\mu\in C} \mathbf{S}_{\lambda\mu}{}^{1/2}\,\mathbf{S}_{\mu\nu}{}^{1/2} \quad (8)$$

where $\mathbf{S}$ is the overlap matrix, and C defines the group of atoms under constraint.

2.2. Forces. The force on nucleus A is the negative of the potential energy gradient at A, which includes the gradients of the nuclear repulsion energy and the electronic energy. Our focus here is the electronic part, whose energy expression is given by eq 3. For a constrained system, the energy is equivalent to the stationary value of W, which is an unconstrained property. Because W is variational with respect to both $\mathbf{P}$ and V_c, using the Hellmann−Feynman theorem and eq 7, we then have

$$\nabla_A W = \nabla_A E + V_c\sum_{\lambda\nu} P_{\lambda\nu}\nabla_A w_{c\lambda\nu} \quad (9)$$

The first term is the gradient in usual unconstrained calculations, which includes the Hellmann−Feynman force, Pulay force,[56] and the force due to the integration grid used in DFT.[57] The second term represents the extra force due to the constraint condition, and it is the part we need to derive.

From eq 8, we have

$$\nabla_A w^L_{c\lambda\nu} = \sum_{\mu\in C}(\mathbf{S}_{\mu\nu}{}^{1/2}\nabla_A\mathbf{S}_{\lambda\mu}{}^{1/2} + \mathbf{S}_{\lambda\mu}{}^{1/2}\nabla_A\mathbf{S}_{\mu\nu}{}^{1/2}) \quad (10)$$

Thus, $\nabla_A\mathbf{S}^{1/2}$ needs to be calculated first. For that, we make use of the eigenvectors and eigenvalues of $\mathbf{S}$, i.e., $\mathbf{C}_i$ and ϵ_i, respectively. After some derivation, one has

$$\nabla_A\mathbf{S}^{1/2} = \sum_{i,j}\frac{\mathbf{C}_i^T\nabla_A\mathbf{S}\mathbf{C}_i}{\sqrt{\epsilon_i}+\sqrt{\epsilon_j}} \quad (11)$$

where T indicates the transpose of a vector. This result can then be used in eq 10 and subsequently in eq 9 to calculate the force in constrained DFT.

We have implemented the above formalism in *NWChem*[58] to calculate the forces of a constrained system and verified its correctness by comparing with gradients computed through finite differences. The forces are then fed into the default driver in *NWChem* for geometry optimization to find the minimum-energy geometry of the constrained diabatic state.

2.3. Driving Force and Inner-Sphere Reorganization Energy. We will use the standard notation $E(a|b)$ to represent the energy of state a calculated at the equilibrium structure of state b, where a and b may or may not be the same. If the two states are DA and D^+A^-, then

$$\Delta G^\circ = E(\mathrm{DA}|\mathrm{DA}) - E(\mathrm{D^+A^-}|\mathrm{D^+A^-}) \quad (12)$$

$$\lambda_i = E(\mathrm{D^+A^-}|\mathrm{DA}) - \mathrm{E}(\mathrm{D^+A^-}|\mathrm{D^+A^-}) \quad (13)$$

The equilibrium structures of both states can be obtained unambiguously with two constrained DFT geometry optimizations. On the other hand, for any fixed structure, constrained DFT provides a direct way to calculate energies of both states. Therefore, the driving force and the reorganization energy are both readily available from constrained DFT. It is instructive to compare eq 13 to the four-point method, which calculates λ_i by

$$\lambda_i^{4p} = [E(\mathrm{D^+}|\mathrm{D}) - E(\mathrm{D^+}|\mathrm{D^+})] + [E(\mathrm{A^-}|\mathrm{A}) - E(\mathrm{A^-}|\mathrm{A^-})] \quad (14)$$

Equation 13 does not separate the donor and the acceptor but fully takes into account their interactions as they are in the real system. This is a clear advantage, especially for intramolecular ET reactions.

It is also useful to compare constrained DFT with usual DFT calculations without constraint. In mixed-valence systems, there are a few systems where unconstrained DFT successfully localizes the unpaired electron and gives ΔG° and λ_i directly.[19,20] However, it is more often the case that DFT fails to localize the unpaired electron because of the overdelocalization problem caused by the self-interaction error (SIE).[59−63] For such cases, DFT cannot distinguish the reactant state and the product state, hence cannot calculate either ΔG° or λ_i. In the case of charge recombination reactions, one of the states is a charge transfer excited state, which is known to be incorrectly described by TDDFT. Taken together, these problems make DFT unsuitable for the vast majority of ET reactions. Constrained DFT does not have these problems, because it can force the unpaired electron to be localized, and it gives a much better description of CT states.[52,53] Therefore, constrained DFT can be a useful tool to study ET reactions, as we demonstrate below.

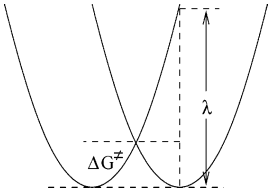

Figure 2. Diabatic potential energy curves for a symmetric electron transfer reaction.

In the following examples, we sometimes attempt to calculate the solvent effects by using the continuum solvent models *COSMO*[64] implemented in *NWChem*. Single-point constrained calculations with *COSMO* are performed at the gas-phase equilibrium structures to approximate total $\Delta G°$. At the current stage, the outer-sphere reorganization energy is not calculated.

3. Calculations and Results

3.1. Tetrathiafulvalene−Diquinone Radical Anion. Our first test is of a symmetric mixed-valence (MV) compound. MV systems have different oxidation states at two redox centers in the same molecule. An unpaired electron may transfer intramolecularly between these two centers. This reaction is also called intervalence transfer (IT), which can be observed optically.[65] For symmetric mixed-valence systems, because the driving force is zero, there are the following simple expressions for the optical ET $\bar{\nu}_{max}$ and the activation energy $\Delta G^{\ddagger}$:[9]

$$\nu_{max} = \lambda = \lambda_i + \lambda_o \tag{15}$$

$$\Delta G^{\ddagger} = \frac{\lambda}{4} \tag{16}$$

Figure 2 demonstrates these relationships.

Robin and Day have divided MV compounds into three classes:[66] Class I has no coupling between the two different states, making the odd electron completely localized at one of the centers. Class II has intermediate coupling; hence though the odd electron is still localized, it can transfer back and forth between the two centers with a small activation energy barrier. Class III has a strong coupling, and the odd electron is completely delocalized over the two centers. DFT calculations have been used to help classify MV compounds. However, the deficiency of overdelocalizing the unpaired electron makes the DFT prediction questionable when a class III compound is assigned. On the other hand, when a class II compound is observed experimentally, DFT may not be suitable to study the system at all.

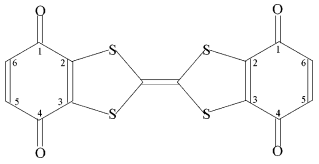

Q-TTF-Q

The symmetric mixed-valence complex tetrathiafulvalene−diquinone (Q-TTF-Q) is synthesized as an example of using TTF as a bridge to conduct electrons between two groups, which may help build electronic devices made of a single molecule.[67] The anion of Q-TTF-Q has been observed by electron spin resonance (ESR) to undergo intramolecular electron transfer,[67] indicating it to be a class II system. However, using the B3LYP functional[68−70] and 6-31+G(d) basis set to optimize the geometry, Q-TTF-Q^- ends up in a symmetric structure, with the two quinone groups having the same amount of charge. (This is true even if we start from an asymmetric structure obtained from constrained DFT below.) Thus, DFT predicts Q-TTF-Q^- to be a class III compound, which does not agree with experiments.

TABLE 1: Comparison of Geometries of the Quinone Groups in Q-TTF-Q^- and Q-TTF-Q, as Well as the Quinone Molecule (Q) and Its Anion (Q^-)[a]

	Q-TTF-Q^-			Q-TTF-Q	Q	Q^-
	DFT	C-neutral	C-reduced			
O−C1	1.246	1.226	1.268	1.226	1.227	1.273
C1−C2	1.464	1.481	1.450	1.481	1.487	1.452
C2−C3	1.370	1.359	1.378	1.359	1.345	1.375
C1−C6	1.470	1.491	1.450	1.489	1.487	1.452
C5−C6	1.358	1.342	1.376	1.343	1.345	1.375
α	168.5	171.4	160.2	166.7		

[a] All bond lengths are in angstroms. C-neutral and C-reduced stand for the constrained DFT results of the neutral and reduced, respectively, Q group geometry in Q-TTF-Q^-.

Figure 3. A side view of the molecular structure of Q-TTF-Q^-. Upper part: DFT results. Lower part: constrained DFT results. Images are produced with VMD.[71]

We can instead explicitly constrain one of the quinones in Q-TTF-Q^- to have one more electron than the other, and then optimize the geometry. The results of this optimization are summarized in Table 1 together with the structures of neutral Q-TTF-Q molecule, quinone, and quinone anion, all using B3LYP/6-31+G(d). The table clearly shows that, in the constrained system, the neutral Q group resembles the structure of the quinone molecule, and the reduced Q group has a similar structure as the quinone anion. The unconstrained DFT results, however, have the Q group geometry close to be the average of the corresponding groups in the constrained DFT results. Note that there is a slight nonplanarity of the Q-TTF-Q structure, resulting from the sp^2 hybridization of the sulfur atoms. In the table, we also list the dihedral angle (α) between the planes of each Q group and the bridge tetrathioethylene group, which can be seen from a side view of the molecule as in Figure 3. It is also interesting to compare the geometry of Q-TTF-Q^- and Q-TTF-Q. The neutral Q group in Q-TTF-Q^- has nearly the same geometry as the Q groups in the neutral Q-TTF-Q molecule. Thus, the reduction of one Q group in Q-TTF-Q does not significantly change the geometry of the other except pushing it further to be coplanar with the bridge group. With the structure of constrained DFT, the inner-sphere reorganization energy, λ_i, is calculated to be 13.08 kcal/mol. The observed IT band is centered around 1300 nm[67] in the 10:1 ethyl acetate/*tert*-butyl alcohol mixture solvent, which means the total reorganization energy is about 22 kcal/mol. Therefore, in this case, λ_i is actually larger than λ_o.

Now, the symmetric structure of Q-TTF-Q^- predicted by DFT is not the correct ground-state geometry, but is there any meaning to this structure? To address this, we performed two

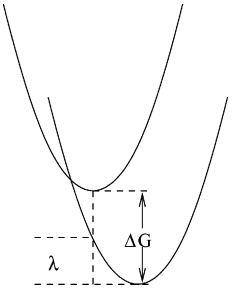

Figure 4. Diabatic potential energy curves for an electron transfer reaction in the inverted region.

constrained calculations at the symmetric structure, with the odd electron either on the left or the right Q group, and found they have the same energy. Furthermore, this energy is 3.31 kcal/mol higher than the minimum constrained state energy, i.e., about one-fourth of λ_i (the true factor is 3.95). These results indicate that the symmetric structure of DFT might be a good approximation of the gas-phase IT transition-state structure of Q-TTF-Q^-. This finding is surprising at first sight, but it is also understandable. Due to symmetry and overdelocalization, the minimum-energy DFT structure has the charge evenly distributed between the two Q groups, which has the same effect as equally mixing the two diabatic states, as it should be for the transition state. Therefore, even though the DFT energy is not reliable at that point, the structure might still be useful. It remains to be tested how useful the overdelocalized DFT structure can be in general for predicting the transition states of mixed-valence complexes.

3.2. Formanilide-Anthraquinone and Ferrocene-Formanilide-Anthraquinone. According to the Marcus theory, there is an inverted region in the ET picture;[13] that is, after some point, the ET reaction rate decreases with increasing driving force. This is the region where the driving force becomes larger than the reorganization energy (Figure 4). The inverted region was not observed experimentally until over two decades after its prediction[72−74] and is one of the greatest triumphs of Marcus theory. Besides the theoretical importance, the inverted region has important practical applications too, and one of those is in the making of a long-lived charge-separated (CS) state.

A long-lived CS state is an essential step in converting light energy to chemical energy in various photoinduced electron transfer processes, such as photosynthesis and photovoltaic cells.[75−77] A long-lived CS state means that the charge recombination reaction is slow compared to other chemical reactions that turn the initial excitation energy stored in the CS state into useful work. One way to obtain a long-lived CS state is to use multiple electron transfer steps to separate the electron and the hole so that they have a small chance to recombine.[78] However, because each step of ET costs some energy, it is preferable to have a long lifetime of the CS state in a single-step ET. This is possible if the CR lies in the inverted region of Marcus theory. An even more attractive quality of the inverted region is that the greater energy stored in the CS state, the slower the CR is.

Recently, a successful case utilizing the inverted behavior in photovoltaic cells has been reported.[79] After laser excitation, the CS state of the formanilide−anthraquinone (FA-AQ) dyad is observed to have a much longer lifetime than that of ferrocene−formanilide−anthraquinone (Fc-FA-AQ) triad (>900 μs compared to 20 ps). It is attributed to a decrease in the driving force and an increase in the reorganization energy, i.e., the charge recombination is in the inverted region. The driving force, as measured electrochemically, is 2.24 eV for FA-AQ and 1.16 eV for Fc-FA-AQ. As an estimation of λ, we make the following derivation from experimental data, in full accordance to the Marcus theory. Assume that the coupling constant H_{ab} is small and the prefactor A in the CR rate expression (eq 2) of both compounds is the same. The ratio of their CS state lifetime then tells the difference of $\Delta G^{\ddagger}$, which is about 0.45 eV. Further assume that the reorganization energy is also the same; then, the total λ is calculated to be 1.41 eV. This simple estimation shows that CR of FA-AQ is in the Marcus inverted region, while that of Fc-FA-AQ is close to the top region.

TABLE 2: Calculated Driving Force and Inner-Sphere Reorganization Energy for the Charge Recombination Reaction of FA-AQ and Fc-FA-AQ[a]

		$-\Delta G_{CR}$ (exptl)	$-\Delta G_{CR}$ (calcd)		
	τ_{CR}		gas phase	in DMSO	λ_i
FA-AQ	>900 μs	2.24	3.25	2.31	0.26
Fc-FA-AQ	20 ps	1.16	2.29	1.02	0.21

[a] Also listed are the experimental driving force and charge-separated state lifetime (τ_{CR}) from ref 79. All energy values are in eV.

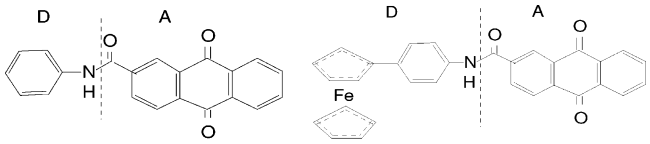

FA-AQ Fc-FA-AQ

We have calculated the driving force and the reorganization energy for the charge recombination of FA-AQ and Fc-FA-AQ in the gas phase, all with the B3LYP functional and the 6-31G(d) basis set. In both compounds, the anthraquinone moiety serves as the electron acceptor. Because the carbonyl group has an electrophilic carbon and the CO double bond conjugates with the anthraquinone, we put the carbonyl group as part of the acceptor too. The rest of the molecule is treated as the electron donor. Our results as well as some experimental data are listed in Table 2. First, examine the gas-phase results. The driving force in both cases is more than 10 times the reorganization energy, showing they are both in the inverted region. FA-AQ and Fc-FA-AQ have similar reorganization energies with only 0.05 eV in difference, but the former has a driving force almost 1 eV larger than the latter (3.25 eV to 2.29 eV). This would agree with the observed trend that FA-AQ has a much longer lifetime of the CS state than Fc-FA-AQ. The fact that the driving force is so much larger (3 or 2 eV) than λ_i suggests that there is a strong possibility that their CR in solution will stay in the inverted region with nonpolar or moderately polar solvents, such as DMSO used in the experiment. (The dielectric constant of DMSO is 46.7.)

To have a better understanding of the solvent effects, we note that the calculated gas-phase driving force is about 1 eV larger than the experimental value measured electrochemically in DMSO solution. This is because a polar solvent stabilizes the CS state more than it does the ground state. We did single-point constrained calculations with the COSMO solvent model. By using a solvent radius of 0.5 Å and dielectric of 46.7, we are able to obtain ΔG values in good agreement with the experiment. From the estimated total λ above, λ_o is about 1.2 eV, which has a much larger contribution than λ.

4. Conclusion

We have further developed the constrained DFT method by presenting an analytic formula for the forces in a constrained

system. Using these forces, we are able to efficiently explore the diabatic potential energy curves in the Marcus theory of electron transfer and make accurate calculations of the driving force and the reorganization energy. Our current implementation gives full account of those parameters for gas-phase reactions. For ET in solution, the inner-sphere reorganization energy can be calculated, and the driving force can be approximated by invoking continuum solvent models.

We wish to summarize a few advantages of using constrained DFT in ET studies. First, constrained DFT provides an easy way to access diabatic states, from which the Marcus parameters can be directly calculated. Second, with constrained DFT, the diabatic states are obtained from ground-state calculations. The difficulty and inaccuracy in excited-state calculations are avoided. Third, with two different constrained geometry optimizations, one naturally obtains the equilibrium structures of both the reactant and product states. The same optimization in adiabatic states guarantees only one equilibrium structure. The last advantage is that the quality of diabatic potential energy curves from constrained DFT is higher than that of the adiabatic curves from DFT. This is because the self-interaction error is more serious for systems with fractional charges.[60] DFT overdelocalizes an unpaired electron, while constrained DFT forces it to be localized. Therefore, the energy values from constrained DFT are more accurate. We note that, because constrained DFT is a ground-state method, it cannot be used for ET reactions that involve a local excited state. However, TDDFT is known to work well for those states.[28,29] A combination of TDDFT and constrained DFT would be a good approach to studying such reactions. We also note that in our method the electron donor and acceptor are preselected. This could be a problem for systems where the donor and the acceptor are not well-separated. Thus, it is clear that at the current stage our method is best for long-range ET reactions, which is what it was developed for.

To make constrained DFT more useful, it is important to calculate the coupling constant, with which accurate adiabatic energies can be obtained from diabatic ones. The coupling constant H_{ab} is crucial in studying nonadiabatic dynamics. DFT overestimates H_{ab}, and one of the consequences is that Robin−Day class III compounds may be falsely assigned. One would like to extend the constrained DFT formalism for obtaining high-quality diabatic energies to also predict accurate H_{ab} values. One of the obstacles is that constrained DFT methods do not produce the real wave function. H_{ab} is the coupling between two different wave functions and has no analogue in terms of static density-dependent observables. Hence, some approximations are necessary to extract H_{ab} from constrained DFT. We are currently performing active research on this topic, and results will be reported in a future work. With H_{ab}, one can also study the issue of degenerate charge transfer states[80] with constrained DFT. In addition, it may be used to work on similar problems addressed by restricted open-shell Kohn−Sham approach.[81,82]

Acknowledgment. This project was funded by an NSF CAREER grant (CHE-0547877).

References and Notes

(1) Gray, H. B.; Winkler, J. R. *Annu. Rev. Biochem.* **1996**, *65*, 537−561.
(2) Cukier, R. I.; Nocera, D. G. *Annu. Rev. Phys. Chem.* **1998**, *49*, 337−369.
(3) Hammes-Schiffer, S. *Acc. Chem. Res.* **2001**, *34*, 273−281.
(4) Grätzel, M. *Nature (London)* **2001**, *414*, 338−344.
(5) Jortner, J., Ratner, M. A., Eds. *Molecular Electronics*; Blackwell Science Ltd.: Oxford, 1997.
(6) Balzani, V., Ed. *Electron Transfer in Chemistry*; Wiley−VCH: Weinheim, 2001.
(7) Marcus, R. A.; Sutin, N. *Biochim. Biophys. Acta* **1985**, *811*, 265.
(8) Marcus, R. A. *Rev. Mod. Phys.* **1993**, *65*, 599.
(9) Barbara, P. F.; Meyer, T. J.; Ratner, M. A. *J. Phys. Chem.* **1996**, *100*, 13148−13168.
(10) Newton, M. D. *Chem. Rev.* **1991**, *91*, 767−792.
(11) Warshel, A.; Parson, W. W. *Annu. Rev. Phys. Chem.* **1991**, *42*, 279.
(12) Marcus, R. A. *J. Chem. Phys.* **1956**, *24*, 966.
(13) Marcus, R. A. *Discuss. Faraday Soc.* **1960**, *29*, 21.
(14) Marcus, R. A. *J. Chem. Phys.* **1965**, *43*, 679.
(15) Small, D. W.; Matyushov, D. V.; Voth, G. A. *J. Am. Chem. Soc.* **2003**, *125*, 7470−7478.
(16) Yeganeh, S.; Ratner, M. A. *J. Chem. Phys.* **2006**, *124*, 044108.
(17) Jortner, J. *J. Chem. Phys.* **1976**, *64*, 4860.
(18) Nelsen, S. F.; Blackstock, S. C.; Kim, Y. *J. Am. Chem. Soc.* **1987**, *109*, 677.
(19) Rosso, K. M.; Smith, D. M. A.; Dupuis, M. *J. Chem. Phys.* **2003**, *118*, 6455.
(20) Rosso, K. M.; Dupuis, M. *J. Chem. Phys.* **2004**, *120*, 7050.
(21) Raubut, G.; Clark, T. *J. Am. Chem. Soc.* **1993**, *115*, 9127.
(22) Tomasi, J.; Persico, M. *Chem. Rev.* **1994**, *94*, 2027.
(23) Cramer, C. J.; Truhlar, D. G. *Chem. Rev.* **1999**, *99*, 2161.
(24) Liu, Y.-P.; Newton, M. D. *J. Phys. Chem.* **1995**, *99*, 12382.
(25) Cossi, M.; Barone, V. *J. Chem. Phys.* **2000**, *112*, 2427.
(26) Yago, T.; Kobori, Y.; Akiyama, K.; Tero-Kubota, S. *J. Phys. Chem. B* **2003**, *107*, 13255−13257.
(27) Casida, M. E. Time-dependent density functional response theory for molecules. In *Recent Advances in Density Functional Methods, Part I*; Chong, D. P., Ed.; World Scientific: Singapore, 1995.
(28) Dreuw, A.; Head-Gordon, M. *Chem. Rev.* **2005**, *105*, 4009.
(29) Burke, K.; Werschnik, J.; Gross, E. *J. Chem. Phys.* **2005**, *123*, 062206.
(30) Tozer, D. J.; Amos, R. D.; Handy, N. C.; Roos, B. O.; Serrano-Andres, L. *Mol. Phys.* **1999**, *97*, 859−868.
(31) Sobolewski, A. L.; Domcke, W. *Chem. Phys.* **2003**, *294*, 73−83.
(32) Fabian, J. *Theor. Chem. Acc.* **2001**, *106*, 199−217.
(33) Dreuw, A.; Weisman, J. L.; Head-Gordon, M. *J. Chem. Phys.* **2003**, *119*, 2943−2946.
(34) Dreuw, A.; Head-Gordon, M. *J. Am. Chem. Soc.* **2004**, *126*, 4007−4016.
(35) McLachlan, A. D. *Mol. Phys.* **1961**, *4*, 417.
(36) Mead, C. A.; Truhlar, D. G. *J. Chem. Phys.* **1982**, *77*, 6090.
(37) Pacher, T.; Mead, C. A.; Cederbaum, L. S.; Köppel, H. *J. Chem. Phys.* **1989**, *91*, 1057.
(38) Smith, F. T. *Phys. Rev.* **1969**, *179*, 111−123.
(39) Baer, M. *Chem. Phys. Lett.* **1975**, *35*, 112.
(40) Baer, M. *Mol. Phys.* **1980**, *40*, 1011.
(41) Macias, A.; Riera, A. *J. Phys. B* **1978**, *11*, L489−L492.
(42) Hendekovic, J. *Chem. Phys. Lett.* **1982**, *90*, 193−197.
(43) Cimiraglia, R.; Malrieu, J. P.; Persico, M.; Spiegelmann, F. *J. Phys. B* **1985**, *18*, 3073.
(44) Pacher, T.; Cederbaum, L. S.; Köppel, H. *J. Chem. Phys.* **1988**, *89*, 7367−7381.
(45) Ruedenberg, K.; Atchity, G. J. *J. Chem. Phys.* **1993**, *99*, 3799.
(46) Domcke, W.; Woywod, C. *Chem. Phys. Lett.* **1993**, *216*, 362−368.
(47) Cave, R. J.; Newton, M. D. *Chem. Phys. Lett.* **1996**, *249*, 15−19.
(48) Nakamura, H.; Truhlar, D. G. *J. Chem. Phys.* **2001**, *115*, 10353−10372.
(49) Dederichs, P. H.; Blügel, S.; Zeller, R.; Akai, H. *Phys. Rev. Lett.* **1984**, *53*, 2512−2515.
(50) Behler, J.; Delley, B.; Lorenz, S.; Reuter, K.; M., S. *Phys. Rev. Lett.* **2005**, *94*, 036104.
(51) Behler, J.; Delley, B.; Reuter, K.; M., S. *Phys. Rev. B*, submitted.
(52) Wu, Q.; Van Voorhis, T. *Phys. Rev. A* **2005**, *72*, 024502.
(53) Wu, Q.; Van Voorhis, T. *J. Chem. Theor. Comput.* **2006**, *2*, 765−774.
(54) Hohenberg, P.; Kohn, W. *Phys. Rev.* **1964**, *136*, B864.
(55) Kohn, W.; Sham, L. *Phys. Rev.* **1965**, *140*, A1133.
(56) Pulay, P. *Mol. Phys.* **1969**, *17*, 197−204.
(57) Johnson, B. G.; Gill, P. M. W.; Pople, J. A. *J. Chem. Phys.* **1993**, *98*, 5612−5626.
(58) High Performance Computational Chemistry Group, *NWChem, A Computational Chemistry Package for Parallel Computers*, version 4.6; Pacific Northwest National Laboratory: Richland, WA 99352, 2004.
(59) Bally, T.; Sastry, G. N. *J. Phys. Chem. A* **1997**, *101*, 7923.
(60) Zhang, Y.; Yang, W. *J. Chem. Phys.* **1998**, *109*, 2604−2608.
(61) Braïda, B.; Hiberty, P. C.; Savin, A. *J. Phys. Chem. A* **1998**, *102*, 7872.
(62) Sodupe, M.; Bertran, J.; Rodriguez-Santiago, L.; Baerends, E. J. *J. Phys. Chem. A* **1999**, *103*, 166.

(63) Blomgren, F.; Larsson, S.; Nelsen, S. *J. Comput. Chem.* **2001**, *22*, 655.
(64) Klamt, A.; Schüurmann, G. *J. Chem. Soc., Perkin Trans.* **1993**, *2*, 799.
(65) Hush, N. S. *Prog. Inorg. Chem.* **1967**, *8*, 391.
(66) Robin, M.; Day, P. *Adv. Inorg. Chem. Radiochem.* **1967**, *10*, 247.
(67) Gautier, N.; Dumur, F.; Lloveras, V.; Vidal-Gancedo, J.; Veciana, J.; Rovira, C.; Hudhomme, P. *Angew. Chem., Int. Ed.* **2003**, *42*, 2765.
(68) Becke, A. D. *Phys. Rev. A* **1988**, *38*, 3098−3100.
(69) Lee, C.; Yang, W.; Parr, R. G. *Phys. Rev. B* **1988**, *37*, 785.
(70) Becke, A. D. *J. Chem. Phys.* **1993**, *98*, 5648−5652.
(71) Humphrey, W.; Dalke, A.; Schulten, K. *J. Mol. Graphics* **1996**, *14*, 33−38.
(72) Miller, J. R.; Calcaterra, L. T.; Closs, G. L. *J. Am. Chem. Soc.* **1984**, *106*, 3047.
(73) McLendon, G.; Miller, J. R. *J. Am. Chem. Soc.* **1985**, *107*, 7811.
(74) Closs, G. L.; Miller, J. R. *Science* **1988**, *240*, 440.
(75) Jordan, K. D.; Paddon-Row, M. N. *Chem. Rev.* **1992**, *92*, 395.
(76) Wasielewski, M. R. *Chem. Rev.* **1992**, *92*, 435.
(77) Bonhôte, P.; Moser, J.; Humphry-Baker, R.; Vlachopoulos, N.; Zakeeruddin, S. M.; Walder, L.; Grätzel, M. *J. Am. Chem. Soc.* **1999**, *121*, 1324−1336.
(78) Gust, D.; Moore, T. A.; Moore, A. L.; Lee, S.-J.; Bittersmann, E.; Luttrull, D. K.; Rehms, A. A.; Degraziano, J. M.; Ma, X. C.; Gao, F.; Belford, R. E.; Trier, T. T. *Science* **1990**, *248*, 199−201.
(79) Okamoto, K.; Hasobe, T.; Tkachenko, N. V.; Lemmetyinen, H.; Kamat, P. V.; Fukuzumi, S. *J. Phys. Chem. A* **2005**, *109*, 4662.
(80) Hieringer, W.; Görling, A. *Chem. Phys. Lett.* **2006**, *419*, 557−562.
(81) Filatov, M.; Shaik, S. *Chem. Phys. Lett.* **1998**, *288*, 689−697.
(82) Filatov, M.; Shaik, S. *J. Chem. Phys.* **1999**, *110*, 116−125.